

Vacuum-Ultraviolet Photoionization Measurement and *ab Initio* Calculation of the Ionization Energy of Gas-Phase SiO₂

Oleg Kostko and Musahid Ahmed*

Chemical Sciences Division, Lawrence Berkeley National Laboratory, Berkeley, California 94720

Ricardo B. Metz

Department of Chemistry, University of Massachusetts, Amherst, Massachusetts 01003

Received: October 16, 2008; Revised Manuscript Received: December 5, 2008

In this work we report on the detection and vacuum-ultraviolet (VUV) photoionization of gas-phase SiO₂ generated *in situ* via laser ablation of silicon in a CO₂ molecular beam. The resulting species are investigated by single-photon ionization with tunable VUV synchrotron radiation and mass analyzed using reflectron mass spectrometry. Photoionization efficiency (PIE) curves are recorded for SiO and SiO₂, and ionization energy estimates are revealed from such measurements. A state-to-state ionization energy of 12.60 ± 0.05 eV is recorded by fitting two prominent peaks in the PIE curve for the following process: $^1\Sigma \text{O-Si-O} \rightarrow ^2\Pi_g [\text{O-Si-O}]^+$. Electronic structure calculations aid in the interpretation of the photoionization process and allow for identification of the symmetric stretch of $^2\Pi_g [\text{O-Si-O}]^+$, which is observed in the PIE spectrum to be 0.11 eV (890 cm^{-1}) above the ground state of the cation and agrees with the 892 cm^{-1} symmetric stretch frequency calculated at the CCSD(T)/aug-cc-pVTZ level.

Introduction

SiO₂ in the solid state is ubiquitous on earth as silica in its various amorphous and crystalline forms and in space in the form of interstellar dust. The importance of silicon-based molecules for the computer industry, optical device manufacture, and recent promise of new chemistry from nanoscale silica has given rise to an enormous scientific literature for SiO₂ in the solid state.^{1–3} However, to date, there has been paucity in the study of SiO₂ in its gaseous state. This stems from the incredible difficulty in generating this species in the gas phase. Brewer and Edwards summarized more than 50 years ago that a mixture of Si and SiO₂ will vaporize to form pure SiO gas and that SiO₂ alone under neutral conditions vaporizes predominantly to SiO and O₂ in the gas phase.⁴ Gas-phase SiO₂ thermodynamics and its vaporization from the solid state is used in many fields ranging from interstellar chemistry^{5–7} to materials science.^{8,9} Mann and Murad¹⁰ discuss the existence of various phases of SiO₂ within the context of formation of Si nanoparticles near the sun, while Schaefer and Fegley¹¹ performed thermodynamic computations to simulate silicate evaporation on Io, one of the moons of Jupiter. Melosh¹² very recently summarized the thermodynamic properties of SiO₂ over extreme pressure and temperature ranges which occur in typical solar system encounters such as the origin of the moon and the extinctions at the end of the Cretaceous era. A rocket-borne experiment suggests that trace amounts of SiO₂⁺ could exist below 100 km in the earth's atmosphere.¹³

There have been few gas-phase mass spectrometry studies in which SiO₂⁺ has been detected. In very early work, Porter et al.¹⁴ using electron impact ionization coupled to high-temperature mass spectrometry on Si/SiO₂ mixtures report appearance energies (AEs) of 10.8 ± 0.5 , 11.7 ± 0.5 , and 10 ± 1 eV for

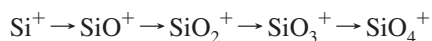
SiO⁺, SiO₂⁺, and Si₂O₂⁺, respectively. By passing heated vapor through an electric quadrupole field and performing mass spectrometry on the resultant oxide cations, Kaufmann et al.¹⁵ postulated that SiO₂ is nonpolar in its neutral ground state. This agrees with IR spectroscopy of matrix-isolated SiO₂^{16–18} in which only one stretch was observed, the antisymmetric stretch ($\nu_3 = 1416 \text{ cm}^{-1}$), which implies that SiO₂ is linear and centrosymmetric. To date these are the only experimental studies to report a vibrational constant for molecular SiO₂.^{16–18} SiO⁺ and SiO₂⁺ signals were observed in electron impact ionization upon heating of SiO₂ with water at 1500 K in an effusion cell.¹⁹ The AEs reported were 11.5 ± 0.3 and 12.0 ± 0.5 eV for SiO⁺ and SiO₂⁺, respectively. The enthalpy of formation $\Delta_f H_{298}^\circ(\text{SiO}_2(\text{g})) = -66.9 \pm 4 \text{ kcal/mol}$ was derived using third-law thermodynamics. This is discrepant with earlier thermodynamic compilations which report $-73 \pm 8 \text{ kcal/mol}$ ²⁰ and $-77 \pm 2.5 \text{ kcal/mol}$.²¹ These numbers are derived from sublimation studies, $\text{SiO}_2(\text{c}) \rightleftharpoons \text{SiO}_2(\text{g})$. Recalculating¹⁹ with an additional reaction channel, $\text{SiO}_2(\text{g}) \rightleftharpoons \text{SiO}(\text{g}) + 1/2\text{O}_2$, provides -66.3 and -68.8 kcal/mol , removing the discrepancy. Allendorf et al.²² report $\Delta_f H_{298}^\circ(\text{SiO}_2(\text{g}))$ to be $-67.4 \pm 2.1 \text{ kcal/mol}$ at the BAC-MP4 level of theory and the bond dissociation enthalpy at 298 K of OSi–O to be 100.1 kcal/mol . Murad²³ tabulates the ionization energy of SiO₂ at 11.5 ± 0.5 eV, presumably from a high-temperature mass spectrometric study. Other high-temperature Knudsen cell experiments report the appearance energy of SiO₂ as 11.5 ± 0.5 eV,²⁴ 12.0 ± 0.5 eV,²⁵ and 11.2 ± 0.2 eV.²⁶

Recently, Reber et al.^{6,7} did not observe SiO₂⁺ directly from laser ablation of solid SiO₂ and SiO, vaporizing Si under oxygen, or by photoionizing the resultant neutral plume using femto-second laser radiation. Using density functional theory, the authors calculated the ionization energy of SiO₂ to be 12.19 eV and suggested that this relatively high energy coupled with a low ionization cross-section did not allow them to observe

* To whom correspondence should be addressed. Phone: (510) 486-6355. Fax: (510) 486-5311. E-mail: MAhmed@lbl.gov.

SiO₂ in the gas phase. These calculations reproduced those of Nayak et al.²⁷ In that work only the geometry of the neutral was reported with a Si–O bond length of 1.53 Å and a binding energy of 8.06 eV to Si + O + O. They also found partial ionic bonding with a net charge of +1.05 on Si and –0.53 on O. There have been a few other theoretical calculations on the molecular properties of gas-phase SiO₂. Harkless et al.²⁸ found a symmetric linear form (*D_{∞h}* geometry) with a 1.46 Å bond length for Si–O, while Pacansky and Hermann²⁹ calculated 1.49 Å as the bond length with similar geometry. They also found that SiO₂ is 4.7 and 6.7 eV bound with respect to SiO(¹Σ⁺) and O(³P) and O(¹D), respectively. Maier et al.³⁰ calculated a triangular O–Si–O structure with *C_{2v}* symmetry (2.45 eV above the linear ground state), a singlet Si–O–O structure with a 170.8° bend in *C_s* symmetry (4.02 eV above the linear ground state), and a triplet Si–O–O structure with a 127.3° bend in *C_s* symmetry (5.15 eV above the linear ground state). Joshipura et al. very recently calculated the electron impact ionization cross-sections for SiO₂.³¹

SiO₂⁺ has been observed in a number of ion–molecule reactions in the laboratory. Fahey et al.³² showed that the ion molecule reaction of Si⁺ with O₂ is an extremely fast three-body reaction which produces excited [O–Si–O]⁺, which efficiently charge transfers with O₂. The authors suggested that most of the excess energy is vibrational in nature. This would suggest that the ionization energy of SiO₂ is above 12.07 eV. Wlodek and Bohme³³ using a selected-ion flow tube (SIFT) showed that oxidation of Si⁺ by N₂O could lead to highly oxygenated systems in the following sequence:



Similar behavior was observed in reactions of laser-generated Si ions trapped in a Fourier transform mass spectrometer.³⁴

Wang³⁵ and co-workers performed a negative ion photoelectron spectroscopic study of SiO₂ and small silicon oxide clusters. They reported a vertical detachment energy of 2.76 eV for SiO₂[–] from a rather broad peak, suggesting that the anion is bent compared to the neutral, which is known to be linear. SiO₂⁺ has been detected upon multiphoton ionization of sputtered neutrals from a SiO₂ surface.³⁶ Very recently, Heinbuch et al.³⁷ measured the mass spectra of silicon oxides among which SiO₂⁺ was present. The oxides were generated in a flow tube reactor in conjunction with laser ablation and photoionized by a 26.5 eV table-top vacuum-ultraviolet (VUV) laser.

We have been successful in generating metals and their oxides^{38,39} and carbon clusters^{40,41} via laser ablation coupled to supersonic molecular beams. Tunable VUV generated at a synchrotron provides a convenient source for single-photon ionization of these species. We applied this method to generate SiO and SiO₂ in the gas phase via reaction of ablated Si with CO₂. Electronic structure calculations were performed to aid in the interpretation of the photoionization results.

Experimental Section

The experiment was performed on a laser ablation apparatus coupled to a 3 m monochromator at the chemical dynamics beamline (9.0.2) at the Advanced Light Source. The apparatus has been described previously.^{38,40} In the original apparatus the ablation rod was rotated and translated by a motor assembly which was located in the source region of the apparatus. For the experiments reported here the motor assembly was outside the apparatus with a vacuum coupling connecting it to the ablation rod inside the source chamber. Attempts to generate SiO₂ in the gas phase by direct laser ablation of quartz and

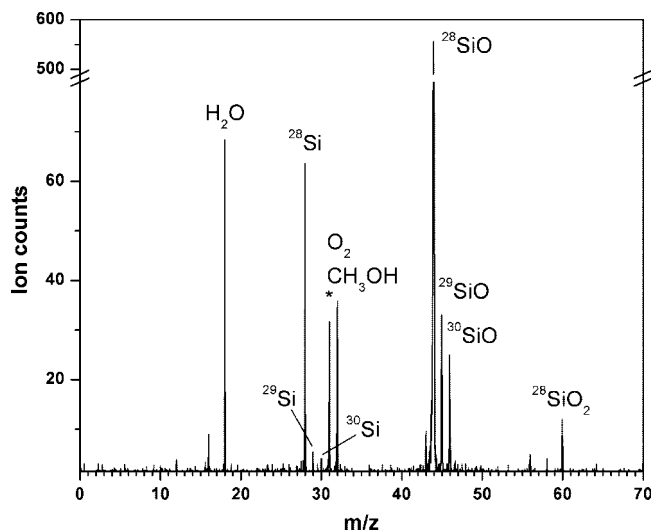


Figure 1. Time-of-flight mass spectrum obtained at a 13 eV photon energy. The asterisk denotes CH₂OH⁺/CH₃O⁺ from dissociative ionization of methanol.

reaction of ablated Si with O₂ and N₂O proved unsuccessful. For the results shown here, SiO₂ was formed by laser ablation of a silicon rod with 532 nm Nd:YAG laser radiation. The resulting Si species were entrained in a beam of pure CO₂ generated via a pulsed valve placed before the ablation rod. Reactions of the ablated plume gave rise to SiO and SiO₂ in the gas phase. Ions formed in the ablation region are removed by deflection plates in the source region. We did not see any evidence of neutral Si(CO₂)_n or SiO(CO₂)_n, although the corresponding cations are observed in a similar source as reported by Jaeger et al.⁴² The ablated beam is skimmed, and in the main chamber, the neutral cluster beam is interrogated in the ionization region of a reflectron time-of-flight (TOF) mass spectrometer by tunable VUV radiation. Since the synchrotron light is quasi-continuous (500 MHz), a start pulse for the TOF ion packet is provided by pulsing the ion optics electric potential. This pulse is synchronized with the ablation laser and pulsed valve timing. The accelerator and repeller plates of the ion optics are biased at the same potential (1200 V), and ions are extracted by fast switching of the repeller plate to 1350 V with a pulse width of 2.5 μs. Ions are accelerated perpendicularly to their initial velocity direction through the field-free region toward the reflectron. Ions, reflected in the electrostatic field of the ion mirror, are detected by a microchannel plate (MCP) installed at the end of the second field-free region. The time-dependent electrical signal from the MCP is amplified by a fast preamplifier, collected by a multichannel-scaler card, and thereafter integrated with a PC computer. Time-of-flight spectra are recorded for the photon energy range between 10 and 13.6 eV. The photoionization efficiency curves of the molecules are obtained by integrating over the peaks in the mass spectrum at each photon energy. The synchrotron VUV photon flux is measured by a Si photodiode. Argon absorption lines are used for energy calibration of the photoionization efficiency (PIE) spectra.

Results and Discussion

A typical mass spectrum recorded at 13 eV photon energy is shown in Figure 1. The most intense peak is ²⁸SiO. ²⁹SiO and ³⁰SiO are also detected, and the ratios between the three Si isotopes correspond to their natural isotopic abundance. The Si atom is detected at *m/z* 28; there is also background H₂O and

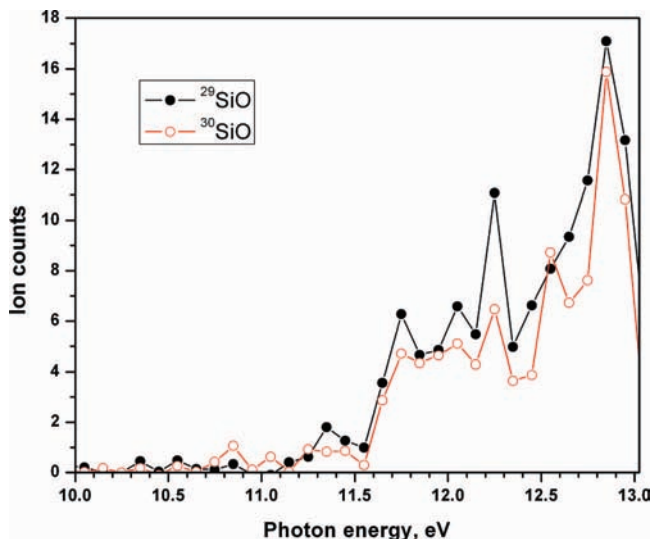


Figure 2. Photoionization efficiency curves for ²⁹SiO and ³⁰SiO recorded with a 100 meV step size with Kr in the gas filter.

O₂ at *m/z* 18 and 32, respectively, and the signal at *m/z* 31 is from dissociative photoionization of methanol. The background signal at *m/z* 31 and 32 arises from methanol remaining in the pulsed valve assembly from a previous experiment. Most importantly, ²⁸SiO₂ is detected at *m/z* 60. Higher masses were not detected in the mass spectrum despite long counting times even though Si clusters are produced in the same source with a different carrier gas (Ar) and laser intensities. The ablation laser energies are different for the case when silicon clusters are produced and when we observe SiO₂, 0.6 and 5.3 mJ per laser pulse, respectively. At a photon energy of 13 eV, the ratio SiO⁺:SiO₂⁺ is ~46, and this ratio will vary with the photoionization cross-section. As has been noted in the Introduction, detection of SiO₂ in the gas phase is very difficult. A quantitative comparison can be made between the results of the mass spectrum shown in Figure 1 and the high-temperature results reported by Porter, Chupka, and Inghram more than 60 years ago. At 1800 K they report an ion current ratio of 281.25 for SiO:SiO₂ which rises to 2250 at 1900 K with a ~17 eV electron impact ionization.¹⁴ Recently, Shornikov et al.²⁶ using electron impact ionization reported similarly high ratios for SiO:SiO₂ of 225 to 53 191 in the temperature range of 1610–1980 K.

Figure 2 shows the photoionization efficiency curve for ²⁹SiO and ³⁰SiO for which we observe a sharp onset at 11.55 eV. At *m/z* 44, there is substantial background from CO₂ (the carrier gas), and hence, a background subtraction has to be employed to retrieve the ionization energy (IE) from the PIE curve of ²⁸SiO. The midpoint of this rise is 11.64 ± 0.05 eV, which agrees well with literature values (11.584 ± 0.011 eV⁴³ from convergence of the Rydberg series, 11.61 eV⁴⁴ from photoelectron spectroscopy), giving us confidence in the quality of the ablation–photoionization experiment. The ion signal observed below the IE could arise from Rydberg states being populated by the VUV photon beam which subsequently field ionize with the extraction pulse in the ionization region of the mass spectrometer. Baig and Connerade⁴³ observed three series of these Rydberg states, (*ns*σ) ¹Σ⁺, (*np*σ) ¹Σ⁺, and (*np*π) ¹Π, converging to the X ²Σ state of SiO⁺. The peak at 12.25 eV arises from excitation to the A ²Π state of SiO⁺, and the 12.85 eV peak arises from population of Rydbergs starting at *n* = 4 (12.739 eV) and converging to the B ²Σ state of SiO⁺.⁴³

Figure 3 shows the photoionization efficiency curve for SiO₂ recorded between 12.05 and 13.20 eV. Six experimental scans

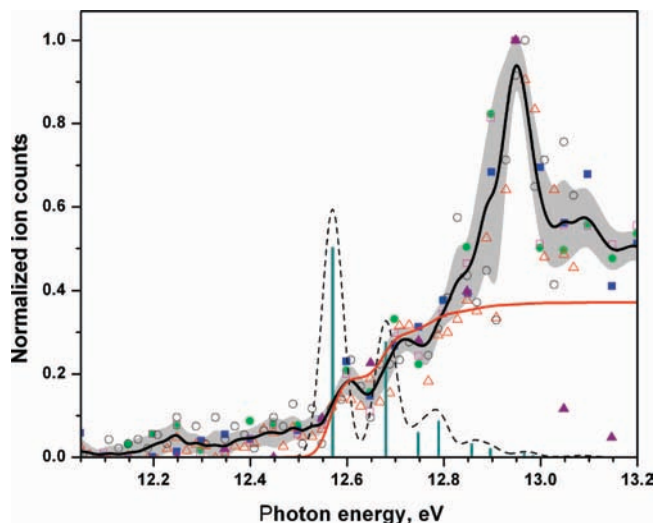


Figure 3. Photoionization efficiency curves for ²⁸SiO₂. The six symbols denote experimental scans. Measurements denoted by the symbols ●, ■, and □ have an experimental photon energy step of 50 meV; the symbols Δ and ○ correspond to a photon energy step of 20 meV. For these five measurements argon was used in a gas filter to filter out higher harmonics of VUV. The symbol ▲ corresponds to a photon energy step of 100 meV and krypton in the gas filter. The solid black line denotes the average of the experimental data obtained using argon in the gas filter. The standard deviation is shown as a wide gray line. Additionally are shown the calculated photoionization efficiency curve as a solid red line, the calculated photoelectron spectrum as dark cyan sticks, and the spectrum broadened by a Gaussian function with a 50 meV width as a black dashed line. The maximal ion signal is normalized to 1.

were conducted during three shifts, and the individual points are color coded in the figure. The average value from these runs is plotted as a continuous black line. Typical step sizes used in these experiments were 20–50 meV. An ion signal appears at 12.15 eV and then gradually rises to 12.55 eV followed by a fairly sharp rise which peaks at 12.6 eV. A second plateau is observed at 12.71 eV followed by a rise which peaks sharply at 12.95 eV. It is very difficult to obtain an ionization energy from the PIE curve shown in Figure 3 since there is no sharp feature at onset, which is typically used to interpret the vertical ionization energy. We turn to theoretical calculations which are described below to guide us in interpreting the SiO₂ PIE.

Electronic structure calculations on SiO₂ and SiO₂⁺ were carried out at several levels of theory using the Gaussian 03 program package.⁴⁵ The SiO₂ molecule is linear and centrosymmetric (OSiO) with a ¹Σ_g ground state at the B3LYP/6-311+G(d) level of theory. It has *r*_{Si-O} = 1.516 Å, with vibrational frequencies ω₂ = 286 cm⁻¹ (bend), ω₁ = 992 cm⁻¹ (symmetric stretch), and ω₃ = 1445 cm⁻¹ (antisymmetric stretch). The centrosymmetric structure and vibrational frequencies are in excellent accord with matrix isolation IR spectroscopy values of 272.5 cm⁻¹ (bend) and 1416.4 cm⁻¹ (antisymmetric stretch).^{16–18} At the same level of theory, for the cation, the ground state is linear, ²Π_g, with *r*_{Si-O} = 1.552 Å and ω_e = 181 cm⁻¹ (bend), 212 cm⁻¹ (bend), 908 cm⁻¹ (symmetric stretch), and 789 cm⁻¹ (antisymmetric stretch). The very low calculated SiO₂⁺ antisymmetric stretch frequency led us to investigate the stretching vibrations of SiO₂ and SiO₂⁺ at the coupled-cluster CCSD(T)/aug-cc-pVTZ level. Single-point energies were computed along each vibrational mode, and vibrational energy levels were calculated by solving the Schrödinger equation numerically. The results for neutral SiO₂ are similar to the B3LYP values: it is centrosymmetric, with *r*_{Si-O} = 1.525 Å and ω₁ =

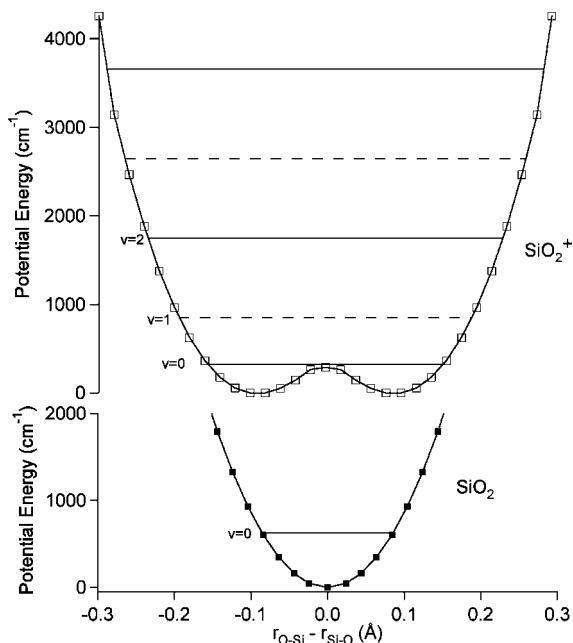


Figure 4. Antisymmetric stretch potentials and vibrational energy levels for SiO_2 and SiO_2^+ . Potentials are calculated at the CCSD(T)/aug-cc-pVTZ level for linear configurations, at $r_{\text{O}-\text{O}} = 3.12 \text{ \AA}$.

970 cm^{-1} (symmetric stretch) and $\omega_3 = 1245 \text{ cm}^{-1}$ (antisymmetric stretch). For SiO_2^+ , the symmetric stretch minimum is at $r_{\text{O}-\text{O}} = 3.12 \text{ \AA}$, and $\omega_1 = 892 \text{ cm}^{-1}$, but the molecule is not centrosymmetric. As shown in Figure 4, the calculation predicts a 290 cm^{-1} barrier, and the vibrational ground state lies above the barrier, at 321 cm^{-1} .

For a transition for a linear OSiO neutral molecule ionizing to a linear OSiO⁺ cation, we calculate 12.57 eV as the ionization energy using both the Gaussian-3⁴⁶ and complete basis set (CBS-QB3)⁴⁷ methods, which have been developed for accurate thermochemistry. This agrees very well with the first sharp peak that we observe in the PIE spectrum at 12.60 eV (Figure 3). The second peak that is observed in the experimental spectrum at 12.71 eV originates from excitation of one quantum in the symmetric stretch of the cation. The 0.11 eV (890 cm^{-1}) spacing agrees with the 892 cm^{-1} symmetric stretch frequency calculated for SiO_2^+ at the CCSD(T) level. For the antisymmetric stretch, ionization of the vibrational ground state of SiO_2 can only produce SiO_2^+ antisymmetric stretch states of even parity. The anharmonic antisymmetric stretch frequencies in the cation are calculated at the CCSD(T)/aug-cc-pVTZ level of theory to have relative energies of 0 cm^{-1} ($\nu_3 = 0$), 1428 cm^{-1} ($\nu_3 = 2$), and 3338 cm^{-1} ($\nu_3 = 4$), respectively. This translates to 12.75 eV ($\nu_3 = 2$) and 12.98 eV ($\nu_3 = 4$) on our energy scale.

We synthesize a photoelectron spectrum at a resolution of 50 meV using the calculated geometries and anharmonic frequencies of the neutral and cation of linear OSiO to better understand the shape of the PIE spectrum that is shown in Figure 3. Integrating the photoelectron spectrum generates a PIE spectrum which is also shown in Figure 3. This is scaled and normalized to the intensity of the first peak at 12.60 eV of the experimental data. As is readily apparent, the synthesized PIE spectrum fits the early part of the spectrum between 12.55 and 12.75 eV very well and reproduces the peak positions of the 0–0 and 0–1 symmetric stretch transitions from the neutral to the cation. This gives us confidence in reporting an error of $\pm 0.05 \text{ eV}$ in the ionization energy determination of SiO_2 . However, it fails to reproduce the peak that is observed at 12.95

eV and the low-energy tail below 12.55 eV seen in the experimental spectrum.

Initially we thought that photoionization from a triangular SiO_2 structure could give rise to the enhanced signal at 12.95 eV and the low-energy tail; however, calculations show that this is not the case. Calculations at the B3LYP/6-311+G(d) level predict that triangular SiO_2 is a local minimum, with C_{2v} symmetry, $r_{\text{Si}-\text{O}} = 1.678 \text{ \AA}$, and $r_{\text{O}-\text{O}} = 1.577 \text{ \AA}$. Triangular SiO_2 is calculated to lie 2.47 eV above the linear isomer at the CBS-QB3 level, in accord with the calculations by Maier et al.³⁰ However, the cation is calculated to have a triangular, C_{2v} structure with $r_{\text{Si}-\text{O}} = 1.810 \text{ \AA}$ and $r_{\text{O}-\text{O}} = 1.354 \text{ \AA}$ that lies only 0.11 eV above the linear isomer. An adiabatic IE (triangular \rightarrow triangular) provides 10.2 eV as the ionization energy, and since there is a substantial geometry change between the triangular neutral and cation, this would lead to a slow onset in the PIE spectrum due to poor Franck–Condon factors. However, the energy range is too low to correlate to our observed PIE spectrum. While the gas-phase spectroscopy of SiO_2 is nonexistent, time-dependent density functional theory (TD-DFT) calculations suggest that the lowest lying electronically excited state is 4.2 eV above the linear ground state. Photoionization of electronically excited SiO_2 would thus also occur at energies too low to contribute to our PIE spectrum. The low-energy onset thus most probably arises from Rydberg states or excited vibrational states which populate the neutral SiO_2 beam in the laser ablation process. We have observed similar effects in the study of carbon clusters using the same source.^{40,41} In that work, low-lying electronically excited states were proposed for the observed low-energy onset. One clue to the fact that SiO_2 being generated in the ablation source could be vibrationally excited, cooling in CO_2 notwithstanding, comes from observations of the reaction of Si^+ with O_2 .³² In that work, it was postulated that insertion into O_2 gives rise to a highly vibrationally excited molecular ion. Insertion of neutral Si into CO_2 in our laser ablation source would also give rise to vibrationally excited species. The process $\text{Si} + \text{CO}_2 \rightarrow \text{C} + \text{SiO}_2$ is 4 eV endothermic and should not directly give rise to SiO_2 in the ablation source. However, $\text{Si} + \text{CO}_2 \rightarrow \text{SiO} + \text{CO}$ is 2.7 eV exothermic, and the subsequent reaction $\text{SiO} + \text{CO}_2 \rightarrow \text{SiO}_2 + \text{CO}$ is 1.1 eV endothermic; the high laser fluencies used in this work should produce excited SiO, which allows the reaction to progress toward SiO_2 formation. Future work, using isotopically labeled molecules, will allow elucidation of the reaction pathways leading to the formation of SiO_2 .

Population of low-lying vibrational states would give rise to a signal in the 12.45 – 12.60 eV region. The sublimation temperature of Si is $\sim 3500 \text{ K}$. This would suggest that the temperature in our ablation source will be at least this temperature since we need Si atoms to prepare SiO_2 . A number of experiments^{48,49} suggest high rotational and vibrational temperatures of SiO species generated in laser ablation of Si in a low-pressure oxygen environment using laser spectroscopy. Hermann et al.⁴⁹ state that the plasma is in a partial local thermal equilibrium and has a temperature of 3500 K . Collisions in the molecular beam under our conditions would lower the temperature, but it is plausible that incomplete cooling would give rise to the low-lying vibrational states and hence lower the appearance energy of SiO_2 .

A prominent feature in the PIE spectrum is the peak at 12.95 eV , or 0.35 eV above the ground state of the cation. TD-DFT calculations were carried out to see whether this feature could be due to transitions to excited electronic states of SiO_2^+ . Neutral linear SiO_2 has the electronic configuration $\dots 0.2\pi_u^4, 4\sigma_u^2, 1\pi_g^4$.

The ${}^2\Pi_g$ ground state of SiO₂⁺ is formed by removing an electron from the $1\pi_g$ orbital. Removing a π_u or σ_u electron leads to the low-lying ${}^2\Pi_u$ and ${}^2\Sigma_u$ states of SiO₂⁺. At the TD-DFT (B3LYP/6-311+G(d)) level, all three states are calculated to be linear and centrosymmetric. The ${}^2\Pi_u$ state is calculated to have $r_{\text{Si-O}} = 1.57$ Å and lie $T_e = 1.20$ eV above the ground state of the cation, while the ${}^2\Sigma_u$ state has $r_{\text{Si-O}} = 1.52$ Å and $T_e = 1.56$ eV. Multiconfigurational self-consistent field (MC-SCF) calculations gave similar excitation energies. Direct ionization to these states does not lead to the 12.95 eV peak, as they lie too high in energy. However, it is likely that this feature arises out of a low-lying Rydberg state that is converging to an electronically excited state of the cation, as is observed for SiO. Also, CO₂ shows several prominent photoionization resonances due to Rydberg series converging to the A ${}^2\Pi_u$ and B ${}^2\Sigma_u$ states of CO₂⁺.⁵⁰ Future studies will also entail photoionization scans to higher energies to explore electronically excited states of SiO₂⁺.

The ionization energy of 12.60 eV determined in this work by fitting the experimental PIE curve to calculated values is a direct determination using photoionization mass spectrometry. Reported appearance energies using electron impact ionization in conjunction with high-temperature mass spectrometry have values between 11.2 ± 0.2 and 12.0 ± 0.5 eV,^{14,24–26} and B3LYP calculations report 12.19 eV.^{6,27} These are all outside the error limits of our work. For the earlier experimental work it is possible that signal-to-noise considerations given the extraordinary difficulty noted in vaporizing SiO₂ coupled with uncertainty in using an extrapolation method in measuring IEs in electron impact studies gave rise to the lower values. A direct comparison to earlier experimental work is not possible since no ionization efficiency curves were published in the literature. However, Porter et al.¹⁴ mention the ratio of ion currents between SiO and SiO₂ at two temperatures in their Knudsen cell. At a 13 eV photon energy, the ratio SiO:SiO₂ is ~46 in our work, which should be contrasted with values of 281.25 (1800 K) and 2250 (1900 K) with an electron impact of ~17 eV reported by Porter et al.¹⁴ and ratios ranging from 225 to 53 191 (1610–1980 K) reported by Shornikov et al.²⁶ This would suggest that, in contrast to high-temperature Knudsen cell experiments, laser ablation coupled with molecular beam entrainment leads to more SiO₂ being formed in the gas phase compared to SiO. This leads us to believe that superior signal-to-noise data in this work and reproducible scans coupled with electronic structure calculations leads to a state to state IE of 12.60 ± 0.05 eV for the following process: ${}^1\Sigma \text{O-Si-O} \rightarrow {}^2\Pi_g [\text{O-Si-O}]^+$. This ionization energy determination allows for comparison of sequential Si-O bond strengths for the neutral and cation for SiO and SiO₂. For the neutral silicon oxides, literature enthalpies of formation $\Delta_f H_{298}^\circ(\text{SiO}_{(g)}) = -23.6$ kcal/mol²¹ and $\Delta_f H_{298}^\circ(\text{SiO}_{2(g)}) = -66 \pm 4$ kcal/mol¹⁹ give bond dissociation enthalpies $D_{298}^\circ(\text{Si-O}) = 191$ kcal/mol and $D_{298}^\circ(\text{OSi-O}) = 103$ kcal/mol. The bond strengths for the ions (obtained using IE(SiO) = 11.61 eV⁴⁴ and IE(SiO₂) = 12.60 eV) are significantly lower: $D_{298}^\circ(\text{Si}^+-\text{O}) = 111$ kcal/mol and $D_{298}^\circ(\text{OSi}^+-\text{O}) = 80$ kcal/mol.

The detection and characterization of SiO₂⁺ in the gas phase reported in this work is a first step toward generation of larger clusters of SiO and SiO₂. Using the same source, Si clusters can be generated up to $n = 7$ using lower laser ablation intensities. With a judicious combination of carrier gas, reagent composition, external cooling of the nozzle source, and laser intensity, it should definitely be possible to probe the elusive gas-phase forms of silica.⁶ Cationic and anionic clusters of SiO

have been detected by various groups;^{6,35,42,51} however, a systematic study of the distribution of neutral SiO and SiO₂ clusters generated via laser ablation has not been performed to date. There is enormous interest in studying, at the molecular level, chemical reactions of water with SiO and SiO₂ in the context of origins of the solar system⁵ and in corrosion and geochemical processes on earth.⁵² Using laser ablation and seeding the carrier gas with water will allow for novel chemistry to be performed within the environs of the source as has been demonstrated in our group recently for reactions of carbon clusters and metal atoms.^{39,53} VUV photoionization coupled with laser ablation promises to be a versatile technique in gaining access to these reaction systems.

Acknowledgment. This work was supported by the Director, Office of Energy Research, Office of Basic Energy Sciences, and Chemical Sciences Division of the U.S. Department of Energy under Contract No. DE-AC02-05CH11231. R.B.M. acknowledges financial support from the National Science Foundation under Award CHE-0608446.

References and Notes

- (1) Teo, B. K.; Sun, X. H. *Chem. Rev.* **2007**, *107*, 1454.
- (2) Jutzi, P.; Schubert, U. *Silicon Chemistry*; Wiley-VCH: Weinheim, Germany, 2007.
- (3) Politi, A.; Cryan, M. J.; Rarity, J. G.; Yu, S.; O'Brien, J. L. *Science* **2008**, *320*, 646.
- (4) Brewer, L.; Edwards, R. K. *J. Phys. Chem.* **1954**, *58*, 351.
- (5) Marcus, R. A. *J. Chem. Phys.* **2004**, *121*, 8201.
- (6) Reber, A. C.; Clayborne, P. A.; Reveles, J. U.; Khanna, S. N.; Castleman, A. W.; Ali, A. *Nano Lett.* **2006**, *6*, 1190.
- (7) Reber, A. C.; Paranthaman, S.; Clayborne, P. A.; Khanna, S. N.; Castleman, A. W. *ACS Nano* **2008**, *2*, 1729.
- (8) Lu, W. C.; Wang, C. Z.; Nguyen, V.; Schmidt, M. W.; Gordon, M. S.; Ho, K. M. *J. Phys. Chem. A* **2003**, *107*, 6936.
- (9) Wang, N.; Cai, Y.; Zhang, R. Q. *Mater. Sci. Eng., R* **2008**, *60*, 1.
- (10) Mann, I.; Murad, E. *Astrophys. J.* **2005**, *624*, L125.
- (11) Schaefer, L.; Fegley, B. *Icarus* **2004**, *169*, 216.
- (12) Melosh, H. J. *Meteorit. Planet. Sci.* **2007**, *42*, 2079.
- (13) Goldberg, R. A. *Radio Sci.* **1975**, *10*, 329.
- (14) Porter, R. F.; Chupka, W. A.; Inghram, M. G. *J. Chem. Phys.* **1955**, *23*, 216.
- (15) Kaufman, M.; Muentner, J.; Klemperer, W. *J. Chem. Phys.* **1967**, *47*, 3365.
- (16) Schnockel, H. *Angew. Chem., Int. Ed. Engl.* **1978**, *17*, 616.
- (17) Schnockel, H. *Z. Anorg. Allg. Chem.* **1980**, *460*, 37.
- (18) Andrews, L.; McCluskey, M. *J. Mol. Spectrosc.* **1992**, *154*, 223.
- (19) Hildenbrand, D. L.; Lau, K. H. *J. Chem. Phys.* **1994**, *101*, 6076.
- (20) Chase, M. W.; Davies, C. A.; Downey, J. R.; Frurip, D. J.; McDonald, R. A.; Syverud, A. N. *J. Phys. Chem. Ref. Data* **1985**, *14*, 1.
- (21) Gurvich, L. V.; Veys, I. V.; Alcock, C. B. *Thermodynamic Properties of Individual Substances*, 4th ed.; Hemisphere: New York, 1989; Vol. 2.
- (22) Allendorf, M. D.; Melius, C. F.; Ho, P.; Zachariah, M. R. *J. Phys. Chem.* **1995**, *99*, 15285.
- (23) Murad, E. *J. Geophys. Res. (Space Phys.)* **1978**, *83*, 5525.
- (24) Zmbov, K. F.; Ames, L. L.; Margrave, J. L. *High Temp. Sci.* **1973**, *5*, 235.
- (25) Wu, C. H.; Ihle, H. R.; Zmbov, K. *J. Chem. Soc., Faraday Trans. 2* **1980**, *76*, 447.
- (26) Shornikov, S. I.; Archakov, I. Y.; Shul'ts, M. M. *Russ. J. Gen. Chem.* **2000**, *70*, 360.
- (27) Nayak, S. K.; Rao, B. K.; Khanna, S. N.; Jena, P. *J. Chem. Phys.* **1998**, *109*, 1245.
- (28) Harkless, J. A. W.; Stillinger, D. K.; Stillinger, F. H. *J. Phys. Chem.* **1996**, *100*, 1098.
- (29) Pacansky, J.; Hermann, K. *J. Chem. Phys.* **1978**, *69*, 963.
- (30) Maier, G.; Reisenauer, H. P.; Egenolf, H.; Glatthaar, J. In *Silicon Chemistry*; Jutzi, P., Schubert, U., Eds.; Wiley-VCH: New York, 2007; p 4.
- (31) Josphura, K. N.; Vaishnav, B. G.; Gangopadhyay, S. *Int. J. Mass Spectrom.* **2007**, *261*, 146.
- (32) Fahey, D. W.; Fehsenfeld, F. C.; Ferguson, E. E.; Viehland, L. A. *J. Chem. Phys.* **1981**, *75*, 669.
- (33) Wlodek, S.; Bohme, D. K. *J. Chem. Soc., Faraday Trans. 2* **1989**, *85*, 1643.

- (34) Creasy, W. R.; Okeefe, A.; McDonald, J. R. *J. Phys. Chem.* **1987**, *91*, 2848.
- (35) Wang, L. S.; Wu, H. B.; Desai, S. R.; Fan, J. W.; Colson, S. D. *J. Phys. Chem.* **1996**, *100*, 8697.
- (36) Wise, M. L.; Emerson, A. B.; Downey, S. W. *Anal. Chem.* **1995**, *67*, 4033.
- (37) Heinbuch, S.; Dong, F.; Rocca, J. J.; Bernstein, E. R. *J. Opt. Soc. Am. B* **2008**, *25*, B85.
- (38) Metz, R. B.; Nicolas, C.; Ahmed, M.; Leone, S. R. *J. Chem. Phys.* **2005**, *123*, 114313.
- (39) Citir, M.; Metz, R. B.; Belau, L.; Ahmed, M. *J. Phys. Chem. A* **2008**, *112*, 9584.
- (40) Nicolas, C.; Shu, J. N.; Peterka, D. S.; Hochlaf, M.; Poisson, L.; Leone, S. R.; Ahmed, M. *J. Am. Chem. Soc.* **2006**, *128*, 220.
- (41) Belau, L.; Wheeler, S. E.; Ticknor, B. W.; Ahmed, M.; Leone, S. R.; Allen, W. D.; Schaefer, H. F.; Duncan, M. A. *J. Am. Chem. Soc.* **2007**, *129*, 10229.
- (42) Jaeger, J. B.; Jaeger, T. D.; Brinkmann, N. R.; Schaefer, H. F.; Duncan, M. A. *Can. J. Chem.* **2004**, *82*, 934.
- (43) Baig, M. A.; Connerade, J. P. *J. Phys. B: At., Mol. Opt. Phys.* **1979**, *12*, 2309.
- (44) Colbourn, E. A.; Dyke, J. M.; Lee, E. P. F.; Morris, A.; Trickle, I. R. *Mol. Phys.* **1978**, *35*, 873.
- (45) Frisch, M. J.; Trucks, G. W.; Schlegel, H. B.; Scuseria, G. E.; Robb, M. A.; Cheeseman, J. R.; Montgomery, J. A., Jr.; Vreven, T.; Kudin, K. N.; Burant, J. C.; Millam, J. M.; Iyengar, S. S.; Tomasi, J.; Barone, V.; Mennucci, B.; Cossi, M.; Scalmani, G.; Rega, N.; Petersson, G. A.; Nakatsuji, H. M.; Hada, Ehara, M.; Toyota, K.; Fukuda, R.; Hasegawa, J.; Ishida, M.; Nakajima, T.; Honda, Y.; Kitao, O.; Nakai, H.; Klene, M.; Li, X.; Knox, J. E.; Hratchian, H. P.; Cross, J. B.; Adamo, C.; Jaramillo, J.; Gomperts, R.; Stratmann, R. E.; Yazyev, O.; Austin, A. J.; Cammi, R.; Pomelli, C.; Ochterski, J. W.; Ayala, P. Y.; Morokuma, K.; Voth, G. A.; Salvador, P.; Dannenberg, J. J.; Zakrzewski, V. G.; Dapprich, S.; Daniels, A. D.; Strain, M. C.; Farkas, O.; Malick, D. K.; Rabuck, A. D.; Raghavachari, K.; Foresman, J. B.; Ortiz, J. V.; Cui, Q.; Baboul, A. G.; Clifford, S.; Cioslowski, J.; Stefanov, B. B.; Liu, G.; Liashenko, A.; Piskorz, P.; Komaromi, I.; Martin, R. L.; Fox, D. J.; Keith, T.; Al-Laham, M. A.; Peng, C. Y.; Nanayakkara, A.; Challacombe, M.; Gill, P. M. W.; Johnson, B.; Chen, W.; Wong, M. W.; Gonzalez, C.; Pople, J. A. *Gaussian 03*; Gaussian, Inc.: Wallingford, CT, Pittsburgh, PA, 2004.
- (46) Curtiss, L. A.; Raghavachari, K.; Redfern, P. C.; Rassolov, V.; Pople, J. A. *J. Chem. Phys.* **1998**, *109*, 7764.
- (47) Montgomery, J. A.; Frisch, M. J.; Ochterski, J. W.; Petersson, G. A. *J. Chem. Phys.* **1999**, *110*, 2822.
- (48) Le, H. C.; Dreyfus, R. W.; Marine, W.; Sentis, M.; Movtchan, I. A. *Appl. Surf. Sci.* **1996**, *96–98*, 164.
- (49) Hermann, J.; Coursimault, F.; Motret, O.; Acquaviva, S.; Perrone, A. *J. Phys. B: At., Mol. Opt. Phys.* **2001**, *34*, 1917.
- (50) Shaw, D. A.; Holland, D. M. P.; Hayes, M. A.; MacDonald, M. A.; Hopkirk, A.; McSweeney, S. M. *Chem. Phys.* **1995**, *198*, 381.
- (51) Garand, E.; Goebbert, D.; Santambrogio, G.; Janssens, E.; Lievens, P.; Meijer, G.; Neumark, D. M.; Asmis, K. R. *Phys. Chem. Chem. Phys.* **2008**, *10*, 1502.
- (52) Zhi, L. L.; Zhao, G. F.; Guo, L. J.; Jing, Q. *Phys. Rev. B* **2008**, *77*, 235435.
- (53) Kaiser, R. I.; Belau, L.; Leone, S. R.; Ahmed, M.; Wang, Y. M.; Braams, B. J.; Bowman, J. M. *ChemPhysChem* **2007**, *8*, 1236.

JP8091495